

Nuclear shape transition at finite temperature in a relativistic mean field approach

B. K. Agrawal¹, Tapas Sil², J. N. De², and S. K. Samaddar¹

⁽¹⁾ Saha Institute of Nuclear Physics, 1/AF,

Bidhannagar, Calcutta - 700064, India

⁽²⁾ Variable Energy Cyclotron Centre, 1/AF,

Bidhannagar, Calcutta - 700064, India

Abstract

The relativistic Hartree-BCS theory is applied to study the temperature dependence of nuclear shape and pairing gap for ^{166}Er and ^{170}Er . For both the nuclei, we find that as temperature increases the pairing gap vanishes leading to phase transition from superfluid to normal phase as is observed in nonrelativistic calculation. The deformation evolves from prolate shapes to spherical shapes at $T \sim 2.7$ MeV. Comparison of our results for heat capacity with the ones obtained in the non-relativistic mean field framework indicates that in the relativistic mean field theory the shape transition occurs at a temperature about 0.9 MeV higher and is relatively weaker. The effect of thermal shape fluctuations on the temperature dependence of deformation is also studied. Relevant results for the level density parameter are further presented.

PACS numbers: 21.10.Ma, 21.60.-n, 27.70.+q

Keywords: Relativistic mean field, Hot nuclei, Shape transition, Level density parameter

I. INTRODUCTION

The relativistic mean field (RMF) theory [1–3] has been very successful in describing the ground state (zero temperature) properties of nuclei over the entire periodic table in recent years. The binding energies, charge radii and the ground state deformations are reproduced very well; the charge distributions also compare extremely well with the experimental data. This theory has proved to be very fruitful in explaining [4–6] various details of exotic nuclei near the drip lines. In contrast to the nonrelativistic models, the RMF theory uses a single set of parameters to explain all these properties. To our knowledge, this approach has not yet been exploited to understand the properties of hot nuclei except some preliminary investigations for closed-shell nuclei [7]. The response of nuclear shapes to thermal excitations, for example, has been experimentally studied from the shapes of the giant dipole resonances (GDR) built on excited states [8,9]. Theoretically such finite temperature effects have been studied till date in the nonrelativistic framework such as the Hartree-Fock-Bogoliubov (HFB) theory [10,11] and the Landau theory of phase transition [12,13]. Such theories qualitatively explain, for example, the temperature evolution of nuclear shapes. Recent experiments indicate, however, that a quantitative estimate of the persistence of the ground state deformation [14] with temperature may be missing in some cases.

Against this backdrop, we undertake the study of the thermal response to nuclear properties, particularly the deformation and the level density in the RMF framework. The HFB calculations employ a model hamiltonian in a limited model space with pairing-plus-quadrupole interaction. This may not be very realistic once temperature comes into play. Moreover, to make the calculations numerically tractable, an inert core is assumed. This may be questionable at moderately high temperatures. The RMF approach we use is effectively free from these limitations. The model space employed is sufficiently large and all the nucleons are treated on equal footing.

In the present work, we employ the nonlinear $\sigma - \omega - \rho$ version of the RMF theory [2].

In absence of a simple relativistic prescription for the pairing interaction, it is introduced phenomenologically. We take two representative systems, namely, ^{166}Er and ^{170}Er . We investigate the thermal evolution of the nuclear shapes and the pairing gaps. The temperature dependence of the specific heat as a possible signature of phase transition in pairing and nuclear shapes is explored. The temperature variation of the nuclear level density parameter which has a pre-eminent role in understanding nuclear reactions is further studied. Effects of thermal fluctuations of the nuclear shapes on the deformation and the nature of the phase transition is also discussed.

The theoretical framework used is briefly discussed in Sec.II. The results and discussions are presented in Sec.III and the Sec.IV contains the concluding remarks.

II. FORMALISM

The Lagrangian density for the nucleon-meson many-body system [2] is taken as

$$\begin{aligned} \mathcal{L} = & \bar{\Psi}_i (i\gamma^\mu \partial_\mu - M) \Psi_i + \frac{1}{2} \partial^\mu \sigma \partial_\mu \sigma - U(\sigma) - g_\sigma \bar{\Psi}_i \sigma \Psi_i \\ & - \frac{1}{4} \Omega^{\mu\nu} \Omega_{\mu\nu} + \frac{1}{2} m_\omega^2 \omega^\mu \omega_\mu - g_\omega \bar{\Psi}_i \gamma^\mu \omega_\mu \Psi_i - \frac{1}{4} \vec{R}^{\mu\nu} \vec{R}_{\mu\nu} + \frac{1}{2} m_\rho^2 \vec{\rho}^\mu \vec{\rho}_\mu \\ & - g_\rho \bar{\Psi}_i \gamma^\mu \vec{\rho}_\mu \vec{\tau} \Psi_i - \frac{1}{4} F^{\mu\nu} F_{\mu\nu} - e \bar{\Psi}_i \gamma^\mu \frac{(1 - \tau_3)}{2} A_\mu \Psi_i. \end{aligned} \quad (1)$$

The meson fields included are the isoscalar σ meson, the isoscalar-vector ω meson and the isovector-vector ρ meson. The arrows in eq. (1) denote the isovector quantities. The Lagrangian contains a nonlinear scalar self-interaction term $U(\sigma)$ of the σ meson:

$$U(\sigma) = \frac{1}{2} m_\sigma^2 \sigma^2 + \frac{1}{3} g_2 \sigma^3 + \frac{1}{4} g_3 \sigma^4. \quad (2)$$

This term is important for appropriate description of the surface properties [15]. The quantities M , m_σ , m_ω and m_ρ are the nucleon, σ , ω and the ρ -meson masses, respectively, while g_σ , g_ω , g_ρ and $e^2/4\pi = 1/137$ are the corresponding coupling constants for the mesons and the photon. The field tensors of the vector mesons and of the electromagnetic fields have the following structure:

$$\Omega^{\mu\nu} = \partial^\mu \omega^\nu - \partial^\nu \omega^\mu, \quad (3)$$

$$\vec{\mathbf{R}}^{\mu\nu} = \partial^\mu \vec{\rho}^\nu - \partial^\nu \vec{\rho}^\mu - g_\rho (\vec{\rho}^\mu \times \vec{\rho}^\nu), \quad (4)$$

$$F^{\mu\nu} = \partial^\mu A^\nu - \partial^\nu A^\mu. \quad (5)$$

The variational principle gives the equations of motion. The mean field approximation is introduced at this stage by treating the fields as c -numbers or classical fields. This results in a set of coupled equations, namely the Dirac equation with potential terms for the nucleons and the Klein-Gordon type equations with sources for the mesons and the photon. For the static case, along with the time reversal invariance and charge conservation the equations get simplified. The resulting equations, known as RMF equations, have the following form. The Dirac equation for the nucleon is

$$\{-i\alpha \cdot \nabla + V(\mathbf{r}) + \beta [M + S(\mathbf{r})]\} \Psi_i = \epsilon_i \Psi_i, \quad (6)$$

where $V(\mathbf{r})$ represents the *vector* potential

$$V(\mathbf{r}) = g_\omega \omega_0(\mathbf{r}) + g_\rho \tau_3 \rho_0(\mathbf{r}) + e \frac{(1 - \tau_3)}{2} A_0(\mathbf{r}), \quad (7)$$

and $S(\mathbf{r})$ is the *scalar* potential

$$S(\mathbf{r}) = g_\sigma \sigma(\mathbf{r}), \quad (8)$$

which contributes to the effective mass as

$$M^*(\mathbf{r}) = M + S(\mathbf{r}). \quad (9)$$

The Klein-Gordon equations for the mesons and the electromagnetic fields with the nucleon densities as sources are

$$\{-\Delta + m_\sigma^2\} \sigma(\mathbf{r}) = -g_\sigma \rho_s(\mathbf{r}) - g_2 \sigma^2(\mathbf{r}) - g_3 \sigma^3(\mathbf{r}), \quad (10)$$

$$\{-\Delta + m_\omega^2\} \omega_0(\mathbf{r}) = g_\omega \rho_v(\mathbf{r}), \quad (11)$$

$$\{-\Delta + m_\rho^2\} \rho_0(\mathbf{r}) = g_\rho \rho_3(\mathbf{r}), \quad (12)$$

$$-\Delta A_0(\mathbf{r}) = e \rho_c(\mathbf{r}). \quad (13)$$

The corresponding densities are

$$\begin{aligned}
\rho_s &= \sum_i n_i \bar{\Psi}_i \Psi_i, \\
\rho_v &= \sum_i n_i \Psi_i^\dagger \Psi_i, \\
\rho_3 &= \sum_i n_i \Psi_i^\dagger \tau_3 \Psi_i, \\
\rho_c &= \sum_i n_i \Psi_i^\dagger \frac{(1 - \tau_3)}{2} \Psi_i.
\end{aligned} \tag{14}$$

Here the sums are taken over the particle states only, i.e., the negative-energy states are neglected. The partial occupancies (n_i) at finite temperature in the constant pairing gap approximation (BCS) is

$$n_i = \frac{1}{2} \left[1 - \frac{\epsilon_i - \lambda}{\tilde{\epsilon}_i} (1 - 2f(\tilde{\epsilon}_i, T)) \right], \tag{15}$$

with $f(\tilde{\epsilon}_i, T) = 1/(1 + e^{\tilde{\epsilon}_i/T})$; $\tilde{\epsilon}_i = \sqrt{(\epsilon_i - \lambda)^2 + \Delta^2}$ is the quasiparticle energy where ϵ_i is the single-particle energy for the state i . The chemical potential λ for protons (neutrons) is obtained from the requirement

$$\sum_i n_i = Z(N) \tag{16}$$

The sum is taken over proton (neutron) states. The gap parameter Δ is obtained by minimising the free energy

$$F = E - TS, \tag{17}$$

where

$$E(T) = \sum_i \epsilon_i n_i + E_\sigma + E_{\sigma NL} + E_\omega + E_\rho + E_C + E_{pair} + E_{CM} - AM, \tag{18}$$

and

$$S = - \sum_i [f_i \ln f_i + (1 - f_i) \ln(1 - f_i)], \tag{19}$$

with

$$E_\sigma = -\frac{1}{2}g_\sigma \int d^3r \rho_s(\mathbf{r})\sigma(\mathbf{r}), \quad (20)$$

$$E_{\sigma NL} = -\frac{1}{2} \int d^3r \left\{ \frac{1}{3}g_2\sigma^3(\mathbf{r}) + \frac{1}{2}g_3\sigma^4(\mathbf{r}) \right\}, \quad (21)$$

$$E_\omega = -\frac{1}{2}g_\omega \int d^3r \rho_v(\mathbf{r})\omega^0(\mathbf{r}), \quad (22)$$

$$E_\rho = -\frac{1}{2}g_\rho \int d^3r \rho_3(\mathbf{r})\rho^0(\mathbf{r}), \quad (23)$$

$$E_C = -\frac{e^2}{8\pi} \int d^3r \rho_C(\mathbf{r})A^0(\mathbf{r}), \quad (24)$$

$$E_{pair} = -\frac{\Delta^2}{G}, \quad (25)$$

$$E_{CM} = -\frac{3}{4}\hbar\omega_0 = -\frac{3}{4}41A^{-1/3}. \quad (26)$$

Here G and A are the pairing strength and the mass number respectively. The single-particle energies and the fields appearing in eqs. (18) - (23) are obtained from the self-consistent solution of eqs. (6) - (12). We generate these self-consistent solutions using the well tested basis expansion method as described in detail in Refs. [2,16].

The self-consistent solutions for the RMF equations at a given temperature is obtained by minimizing the free energy F which yields the equilibrium or the most probable value of the quadrupole deformation (β_2^0) and the proton (neutron) pairing gaps Δ_p (Δ_n). To incorporate the effects of the thermal fluctuations, a constrained calculation is performed to generate the free energies for the deformations away from the equilibrium value. Average value of a quantity then can be obtained as

$$\bar{O} = \frac{\int d\beta_2 O(\beta_2) e^{-\Delta F(\beta_2)/T}}{\int d\beta_2 e^{-\Delta F(\beta_2)/T}} \quad (27)$$

where $\Delta F = F(\beta_2) - F(\beta_2^0)$ and $O(\beta_2)$ is the expectation value of the operator \hat{O} at a fixed value of β_2 and T . The quantity $e^{-\Delta F/T}$ is a measure of the probability for the nucleus to have deformation β_2 at the temperature T .

III. RESULTS AND DISCUSSIONS

We have chosen ^{166}Er and ^{170}Er as two representative systems for our calculations. The results presented are obtained using the NLSH parameter set [16] for the values of the

coupling constants and masses for the mesons and nucleons. The pairing strength G is taken to be $29/A$ and $21/A$ for protons and neutrons, respectively; they reasonably reproduce the observed pairing gaps at zero temperature obtained from odd-even mass differences. The values of the chemical potential and the pairing gap are determined using all the single particle states up to $2\hbar\omega_0$ above the Fermi surface without assuming any core, i.e., the mean field solution is generated by taking into account all the nucleons in the systems considered.

At finite temperatures, the nucleus is not strictly in thermal equilibrium. In order to treat the system as an isolated one in equilibrium, one has to take into account corrections due to excitations of nucleons in the continuum. This is generally done through a subtraction procedure, by treating the liquid plus vapour phase together and then the vapour phase separately [17]. However, calculations of the nuclear level density parameter at finite temperature show that the results are insensitive [18] to the continuum corrections for T upto ~ 3 MeV; we have therefore not included the effects due to the continuum in the present calculations as temperatures above it are not relevant.

In subsec.3.1, the results for the most probable values (i.e, the mean field values) of the different observables are presented. With increasing temperature, thermal fluctuations build up which may shift the average values from the most probable ones. In subsec.3.2, we discuss the results with the inclusion of thermal fluctuations. Fluctuations in both the β_2 and γ - degrees of freedom of the nuclear shape should be incorporated, however, because of simplicity and computational economy, we have included only the β_2 - fluctuations in the present calculations.

A. Mean field results

We have calculated the most probable values of the quadrupole deformation parameter, neutron and proton pairing gaps, heat capacity and the level density parameters for the aforesaid systems as a function of temperature.

In Fig. 1, the variation of the quadrupole deformation parameter β_2 as a function of

temperature is shown. The ground state deformations obtained here are almost close to the ones calculated in Refs. [10,11] using nonrelativistic mean field theory with pairing plus quadrupole (P+Q) interaction. The nature of the temperature dependence of the deformation in the two cases are also not very different. However, whereas in the nonrelativistic case the phase transition from prolate to spherical shape occurs at $T \sim 1.8$ MeV, in the present case the said transition is found at a higher temperature, $T \sim 2.7$ MeV. The signature of the phase-transition can be inferred by examining other observables like heat capacity which we consider later.

In Fig. 2, the results for the evolution of the neutron and proton pairing gaps with temperature are displayed. For both the nuclei the pairing gaps monotonically decrease with the increase in temperature. It is seen that for both the nuclei, the neutron pairing gaps vanish almost at the same temperature $T \sim 0.4$ MeV; similarly the proton pairing gaps vanish at $T \sim 0.45$ MeV. These results are not much in variance with those obtained in the nonrelativistic P+Q model.

The vanishing of the nuclear deformation and the pairing gaps with temperature indicates that there is a shape transition from prolate to spherical and also a transition from the superfluid phase to the normal phase. To understand the nature of the transitions, the heat capacity at various temperatures are calculated. The specific heat C for a given temperature is obtained using

$$C(T) = \frac{\partial E^*}{\partial T} \quad (28)$$

where E^* is the excitation energy of the nucleus. In Fig. 3, the temperature variation of the specific heat for ^{166}Er and ^{170}Er nuclei is plotted. At $T \sim 0.4$ MeV, two closely separated peaks in the $C(T)$ curves are seen. They correspond to the dissolution of the neutron and proton pairing gaps. These are the characteristic signatures of second order phase transitions from superfluid to normal phase. It is further noted that the heat capacities for the two systems have broad bumps at $T \sim 2.7$ MeV. This signifies a weak second order phase transition corresponding to the transition of the nuclear shape. This result is at variance

with those obtained in the P+Q model or in the nonrelativistic calculation [12] based on the Landau theory of phase transitions where a strong second order phase transition is observed.

We now present the results for the temperature dependent level density parameter a . The parameter a can be obtained using the excitation energy and the entropy as follows,

$$E^* = aT^2, \quad (29)$$

$$S = 2aT. \quad (30)$$

The parameter a obtained using above eqs. (29) and (30) would be equal provided it is independent of temperature [19]. In Fig. 4, the inverse level density parameter $K = A/a$ (A is the mass number of the nucleus) is plotted as a function of temperature. The subscripts E and S are used to distinguish the two definitions given by eqs. (29) and (30), respectively. At lower temperature, both K_E and K_S shoot up due to the collapse of the pairing gaps. At higher temperatures, K_E and K_S are quite close to each other and there is no appreciable variations in their values in the temperature range considered. This is due to the weak transition of the nuclear shapes from deformed to spherical at $T \sim 2.7$ MeV.

In order to test the sensitivity of the results presented above to the choice of the parameter set and the model space, we have repeated the calculations for the nucleus ^{166}Er with the NL3 parameter set [20,21]. In comparison to the results for NLSH parameter set it is found that the NL3 parameter set gives slightly larger ($\sim 10\%$) value of the ground state deformation. For $T > 1.5$ MeV, the values of deformation obtained in both NLSH and NL3 parameter sets are almost identical. The temperature evolution of the pairing gaps and level density parameters are practically the same with the two parameter sets. We extend the model space to include single particle states upto $3\hbar\omega_0$ above the Fermi surface instead of $2\hbar\omega_0$ as used above. For this extended model space the pairing strength G is adjusted to reproduce the ground state pairing gap. We do not find significant changes in the values of deformation parameter and the pairing energy in the temperature range of interest ($T \sim 3$ MeV). In the extended model space, the value of the inverse level density parameter is also nearly the same. The model space used is thus found to be sufficient for our calculations. To

estimate the importance of the continuum corrections to the inverse level density parameter we calculated the occupancy, $n^{(+)}$, of the single-particle states with positive energy. For $T < 1$ MeV practically there is no particle in the positive energy states ($n^{(+)} = 0$) and at the highest temperature of interest studied $n^{(+)}/A = 0.018$ which is very small. Thus it is expected that the continuum corrections may not play an important role in the temperature range we study. The continuum effects may grow stronger for $T > 3$ MeV, however, this is beyond the transition temperatures and so we have not taken this into account.

The shape transition temperature and the inverse level density parameter obtained in the present model are higher compared to those calculated in the (P+Q) model [10,11]. Moreover, in the later model, the deformation falls to zero sharply whereas in the present case, this fall is comparatively a little slower. The origin of these differences can be attributed to the single-particle level spectra. In Fig.5, the energy levels for the different proton orbitals around the Fermi surface for the nucleus ^{170}Er at $T=3.0$ MeV are displayed. Also the proton single-particle energies in the (P+Q) model are shown at this temperature. In both models the orbits are spherical at this temperature. The striking difference between the orbitals in the two models is the large energy gap across the Fermi surface in the RMF model. Similar is the case for neutrons. These tend to reduce the entropy and the excitation energy and hence the level density parameter. The increase in the shape transition temperature (by ~ 0.9 MeV) in the RMF model as compared to the P+Q model may be traced back to the specific level structure and the gap across the Fermi surface in the two models and their thermal response.

B. Results with thermal fluctuations

Experimental data on giant dipole resonances built on excited states give estimates of the average values of nuclear deformation at finite temperatures. They can be calculated by taking into account the thermal fluctuation effects around the 'most probable' value. Nuclei being finite systems, one expects that thermal fluctuations would play an important

role in the quantitative estimation of various nuclear observables at finite temperatures. In fact, it has been shown in Ref [22] that the experimental data on GDR built on the excited states can be explained reasonably only if the effects from the thermal fluctuations of all the quadrupole degrees of freedom for nuclear shape are included. In the following, we consider the thermal fluctuations only in the β_2 degree of freedom. Inclusion of fluctuations in the γ -degrees of freedom is very involved and computer-intensive and therefore not considered presently. We perform constrained calculations for free energy at fixed deformations β_2 . The free energy surface shows multiple minima for temperatures below the shape transition temperature. The average value of β_2 is calculated using eq.(27). In Fig.6, we have displayed the plots of free energy surface ΔF for ^{170}Er at a few temperatures ranging from 2.0 to 3.0 MeV where ΔF is measured from the lowest minimum (prolate in the present case) at the corresponding temperature. For $T = 2.0$ MeV, the free energy surface has minima at $\beta_2 = -0.16$ and 0.23. The free energy difference between these two minima is 0.70 MeV (i.e. $\Delta F/T = 0.35$). As the temperature approaches the shape transition temperature ($T \sim 2.7$ MeV), both the minima in the free energy surface merge and flatten the bottom part of the free energy surface. This is evident from the middle panel of Fig.6 corresponding to $T = 2.65$ MeV. With further increase in temperature, the free energy surface with single minimum at zero deformation broadens. The variation of the average deformation ($\bar{\beta}_2$) as a function of temperature obtained through eq.(27) for ^{170}Er is shown in Fig.7. The average value of β_2 differs significantly from its most probable value (see Fig. 1) for temperatures above 1 MeV. The reason for such differences can be understood as follows. The free energy surface for ^{170}Er at low temperatures ($T < 2$ MeV) shows two well separated minima. One of these minima lies at prolate deformation (F_p) and the other one is at oblate deformation (F_o). Their difference $\Delta F^0 = F_o - F_p$ as a function of temperature is shown in Fig.8. For $T > 0.5$ MeV, ΔF^0 decreases monotonically to zero. The initial rise of ΔF^0 can be attributed to the quenching of the pairing correlations; it is seen that without pairing, ΔF^0 decreases uniformly with temperature. The decrease in ΔF^0 enhances the probability of finding the nucleus with oblate deformation and hence the average deformation is smaller than the

most probable one for temperatures below the transition temperature. The deviation of the average deformation from the most probable value is also governed by $\Delta\beta_2 = \beta_2^p - \beta_2^o$. Here, β_2^p and β_2^o are the deformations corresponding to the prolate and the oblate minima. With rise in temperature, they come closer and ultimately merge as shown in Fig. 9. The persistence of $\bar{\beta}_2$ beyond the transition temperature is attributed to the asymmetry in the free energy surface as seen in the bottom panel of Fig.6. A similar behavior for ^{166}Er is also seen.

In the mean field approximation, the thermal evolution of the most probable value of the deformation is seen to be associated with two phase transitions, the first being a superfluid phase to normal phase transition at $T \sim 0.4$ MeV and the other a weak second order phase transition in the shape at $T \sim 2.7$ MeV. It would be interesting to see how thermal fluctuations affect these phase transitions. In Fig. 10, the specific heat for the system ^{170}Er is displayed as a function of temperature with inclusion of fluctuations. At low temperatures for $T < 1.0$ MeV, there is no perceptible change in the specific heat and thus the transition from superfluid to normal phase is not affected by fluctuations. At a little higher temperature, however, the broad bump seen in Fig.3 at ~ 2.7 MeV is seen to be shifted to ~ 1.6 MeV and becomes also a little sharper. The phase transition in nuclear shape thus occurs at a lower temperature and is not as weak as seen in the mean field approximation. Normally, one would expect the phase transition to get diluted due to presence of fluctuations. Here one sees the opposite. The evolution of the free energy and the energy profiles with temperature showing two minima (one prolate and the other oblate) in deformation space is responsible for this observation. Here the role of thermal fluctuations becomes significant only in the intermediate temperature domain (temperature in the range 1 - 2.5 MeV, approximately) due to decrease in ΔF^0 and $\Delta\beta_2$ (see Figs. 8 and 9). The delicate interplay of these quantities in the averaging augurs a change in the heat capacity signalling a somewhat sharper shape transition at a lower temperature compared to the most probable one.

The effect of thermal fluctuations of the shape coordinate β_2 on the inverse level density parameter K for the system ^{170}Er is shown in Fig.11. The full line and the dashed line

correspond to results of our calculations for K_S and K_E , respectively. The corresponding lines with circles represent those with inclusion of the fluctuations. It is seen that the fluctuations shift the minima for K_S and K_E from 2.7 MeV to 1.6 MeV, the corresponding transition temperature. Beyond the transition temperature, the upward slope for K is also found to be higher with fluctuations included. Similar is the behavior for ^{166}Er .

IV. CONCLUSIONS

The relativistic mean-field approach together with pairing effects included through the constant gap approximation has been applied to study some properties of axially deformed ^{166}Er and ^{170}Er nuclei at finite temperature. The temperature dependence of the quadrupole shape for both the nuclei are found to be practically the same; similar is the case for the pairing gaps. The deformation remains close to its ground state value ($\beta_2 \sim 0.3$) for T less than 1.5 MeV and falls to zero quite sharply at $T \sim 2.7$ MeV. Pairing gaps vanish at $T = 0.4 - 0.5$ MeV leading to transition from a superfluid phase to normal phase. Compared with the results obtained in the nonrelativistic mean field framework, the relativistic calculations yield vanishing pairing gaps at practically the same temperature and the fall is a bit slower. The evolution of the heat capacity with temperature and the transition from superfluid to normal phase do not behave very differently. The nature of the shape transition obtained in the two approaches are also not too different except that in the present case, the approach of the deformation to zero is relatively slower. This slower fall results in a broad bump in the specific heat around the shape transition temperature ($T \sim 2.7$ MeV).

Fluctuations are expected to influence the phase transitions. To explore these aspects, we have taken into consideration thermal fluctuations in the β_2 - degrees of freedom. The effects of fluctuations are found to be imperceptible below $T \sim 1$ MeV and therefore the pairing transitions are not affected. However, the influence on the shape transitions is found to be very significant; the transition temperature drops down from ~ 2.7 MeV to ~ 1.6 MeV with inclusion of thermal fluctuations. It also becomes a little sharper. The specific nature

of the free energy surface in the deformation space and its evolution with temperature are responsible for such a behavior. Fluctuations in the γ - degrees of freedom would also have a role to play in the phase transitions mentioned. We have not included these presently as they are computationally too intensive.

The authors gratefully acknowledge Prof. P. Ring for providing them with the computer code to generate RMF solutions for axially deformed nuclei at zero-temperature.

REFERENCES

- [1] B. D. Serot and J. D. Walecka, *Adv. Nucl. Phys.* **16**, 1 (1986).
- [2] Y. K. Gambhir, P. Ring and A. Thimet, *Ann. Phys. (N.Y.)* **198**, 132 (1990).
- [3] P. Ring, *Prog. Part. Nucl. Phys.* **37**, 193(1996).
- [4] D. Vretenar, G. A. Lalazissis and P. Ring, *Phys. Rev. Lett.* **82**, 4595 (1999).
- [5] W. Poeschl, D. Vretenar, G. A. Lalazissis and P. Ring, *Phys. Rev. Lett.* **79**, 3841(1997).
- [6] G. A. Lalazissis, D. Vretener, W. Poeschl and P. Ring, *Nucl. Phys.* **A632**, 363 (1998).
- [7] Y. K. Gambhir, *Proc. of the topical meeting on nuclear fragmentation, Calcutta, India*, P101 (1989).
- [8] K. A. Snover, *Annu. Rev. Nucl. Part. Sc* **36**, 545 (1986).
- [9] J. J. Gaardhoje, *Annu. Rev. Nucl. Part. Sc.* **42**, 483 (1992).
- [10] A. L. Goodman, *Phys. Rev.* **C34**, 1942 (1986).
- [11] A. L. Goodman, *Phys. Rev.* **C38**, 977 (1988).
- [12] Y. Alhassid, S. Levit and J. Zingman, *Phys. Rev. Lett.* **57**, 539 (1986).
- [13] Y. Alhassid, J. Zingman and S. Levit, *Nucl. Phys.* **A469**, 205 (1987).
- [14] M. P. Kelley, K. A. Snover, J. P. S. van Schagen, M. Kicinska- Haboir and Z. Trznadel, *Phys. Rev. Lett.* **82**, 3404 (1999).
- [15] J. Boguta and A. R. Bodmer, *Nucl. Phys.* **A292**, 413 (1977).
- [16] P. Ring, Y. K. Gambhir and G. A. Lalazissis, *Comp. Phys. Comm.* **105**, 77 (1997).
- [17] P. Bonche, S. Levit and D. Vautherin, *Nucl. Phys.* **A436**, 265 (1985).
- [18] B. K. Agrawal, S. K. Samaddar, A. Ansari and J. N. De, *Phys. Rev.* **C59**, 3109 (1999).

- [19] B. K. Agrawal, S. K. Samaddar, J.N.De and S. Shlomo, Phys. Rev. **C58**, 3004 (1998).
- [20] G. A. Lalazissis, D. Vretenar and P. Ring, Phys. Rev. **C57**, 2294 (1998).
- [21] G. A. Lalazissis and P. Ring, Phys. Lett. **B427**, 225 (1998).
- [22] Y. Alhassid and B. Bush, Phys. Rev. Lett.**65**, 2527 (1990).

Figure Captions:

- Fig. 1: Variation of the most probable quadrupole deformation β_2 as a function of temperature for ^{166}Er and ^{170}Er .
- Fig. 2: Temperature evolution of neutron and proton pairing gaps for ^{166}Er and ^{170}Er .
- Fig. 3: Variation of specific heat as a function of temperature for ^{166}Er and ^{170}Er .
- Fig. 4: Temperature dependence of inverse level density parameters K_E and K_S determined from the excitation energy and the entropy, respectively.
- Fig. 5: Spectra of the proton single-particle energies around the Fermi surface for ^{170}Er at $T = 3.0$ MeV in the RMF and the (P+Q) models. The single-particle energies ϵ are shown relative to the respective chemical potentials.
- Fig. 6: Plots for the free energy surface at various temperatures for ^{170}Er . The free energies at different temperatures are measured from the respective lowest minimum.
- Fig. 7: Average value of quadrupole deformation as a function of temperature for ^{170}Er .
- Fig. 8: The free energy difference between the prolate and the oblate minima as a function of temperature for ^{170}Er .
- Fig. 9: The difference $\Delta\beta_2$ between the deformations at the prolate and the oblate minima as a function of temperature for ^{170}Er .
- Fig. 10: Variation of average specific heat as a function of temperature for ^{170}Er .
- Fig. 11: The inverse level density parameter for the system ^{170}Er . The full and the dashed lines correspond to K_S and K_E , respectively. The lines with filled circles represent the corresponding results with inclusion of thermal fluctuations.

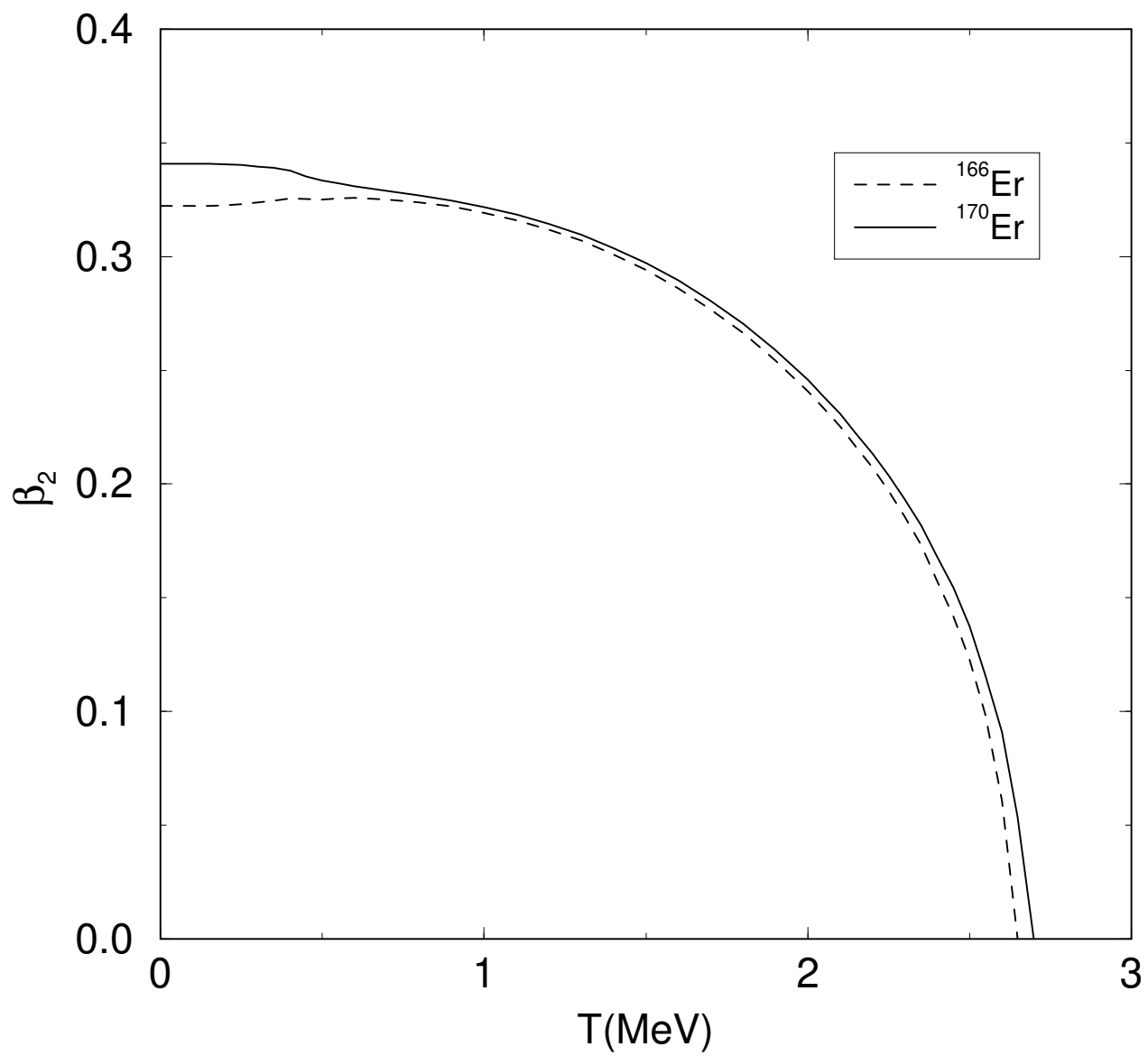


Fig. 1

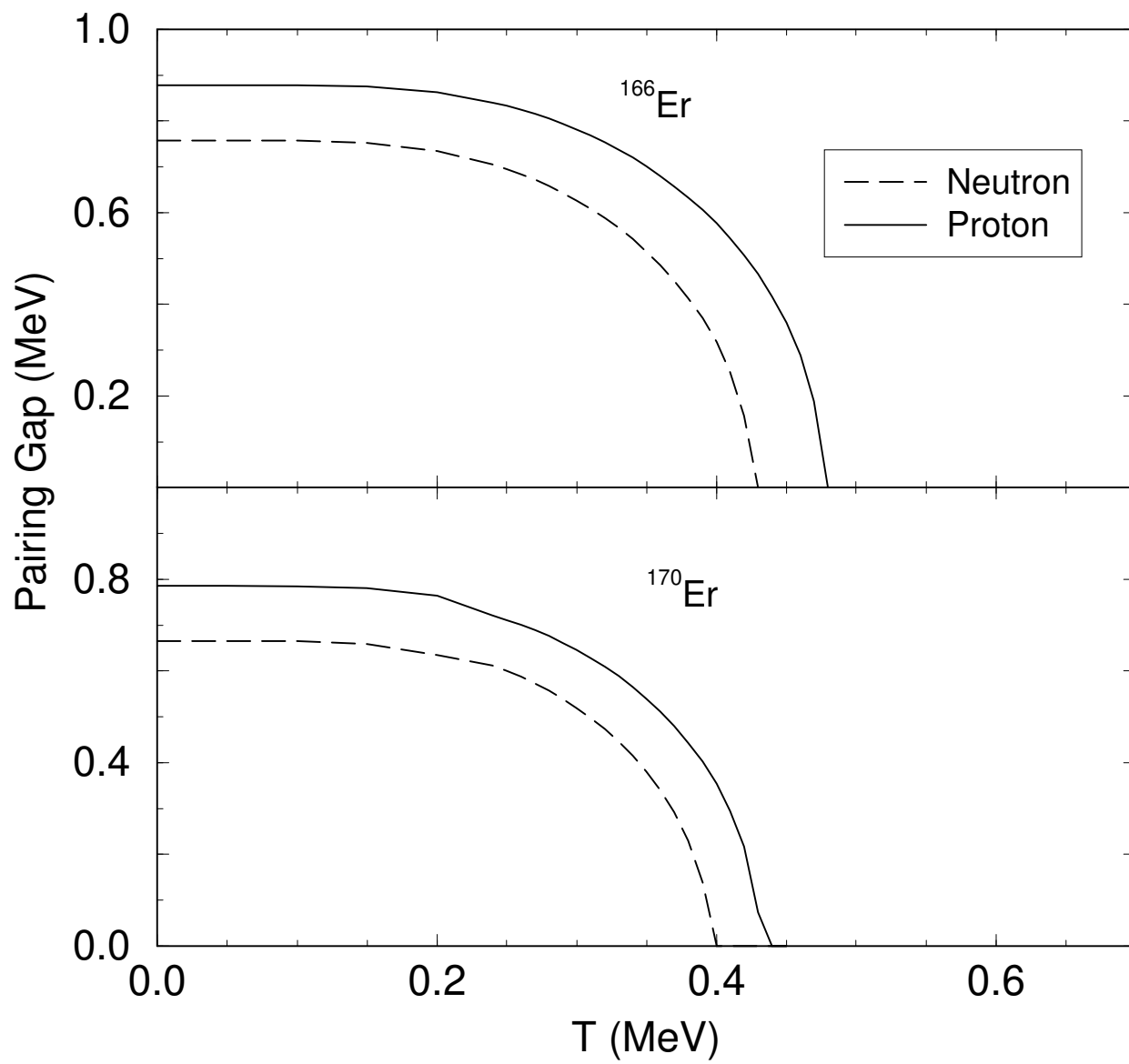


Fig. 2

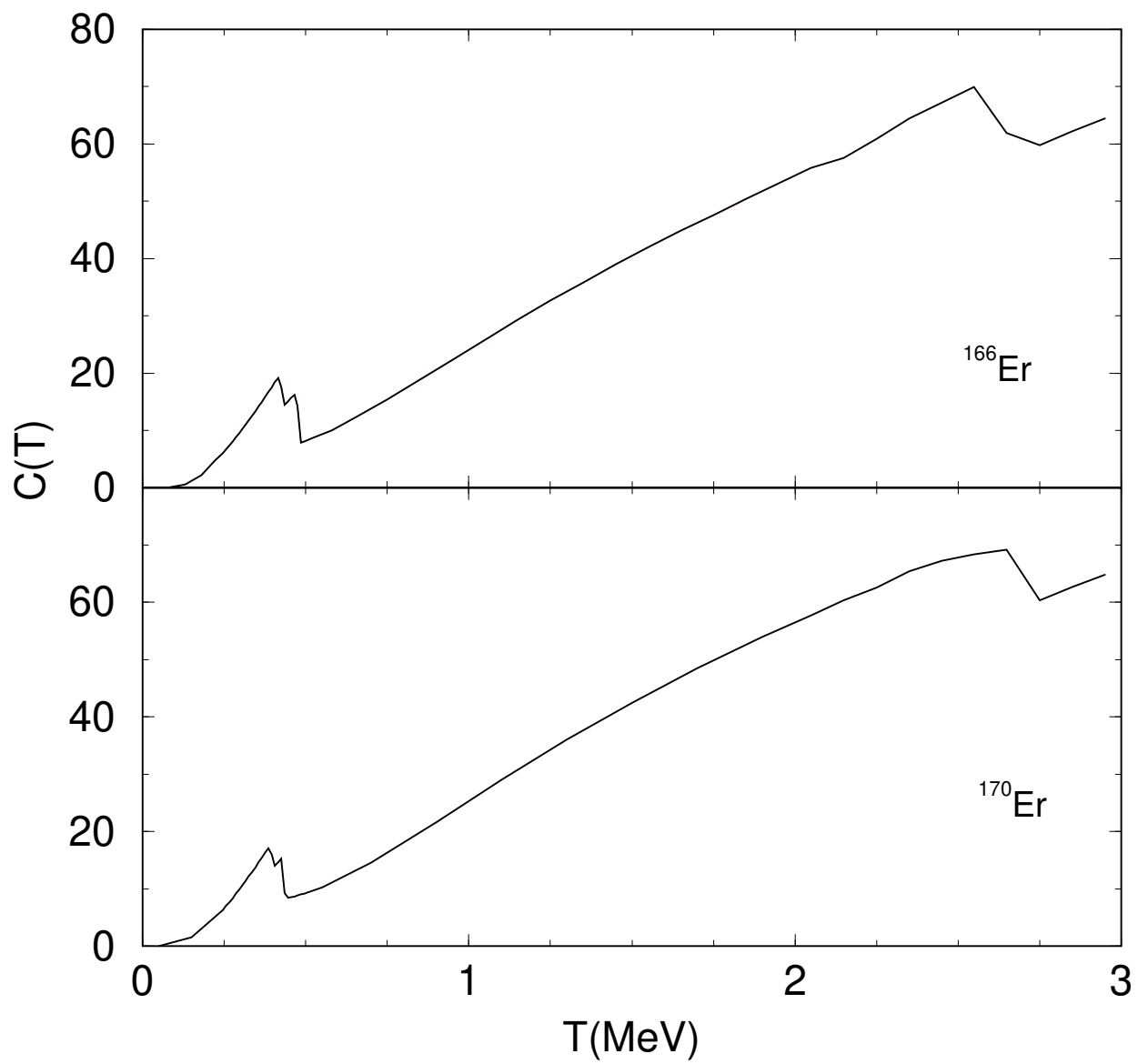


Fig. 3

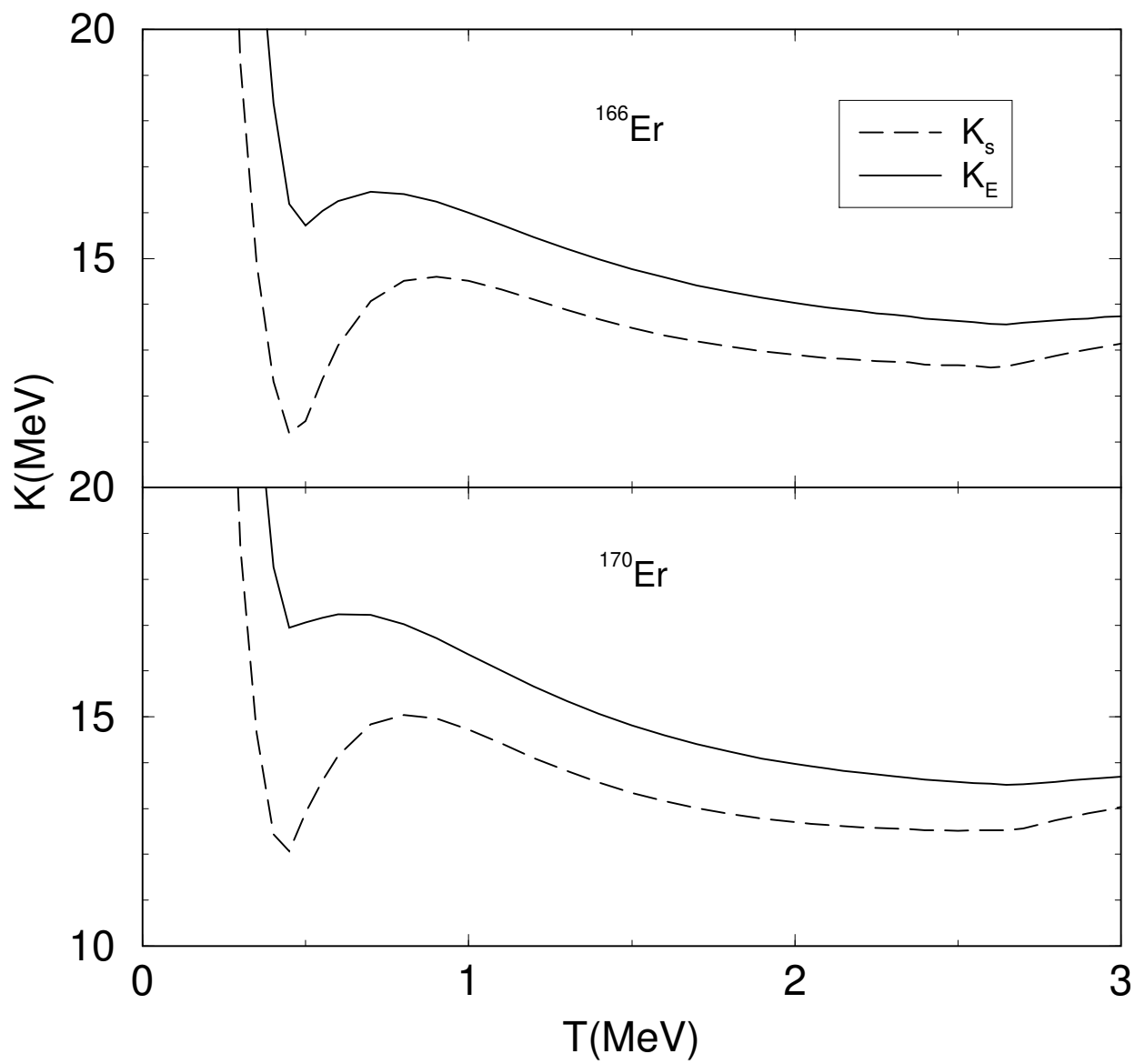


Fig. 4

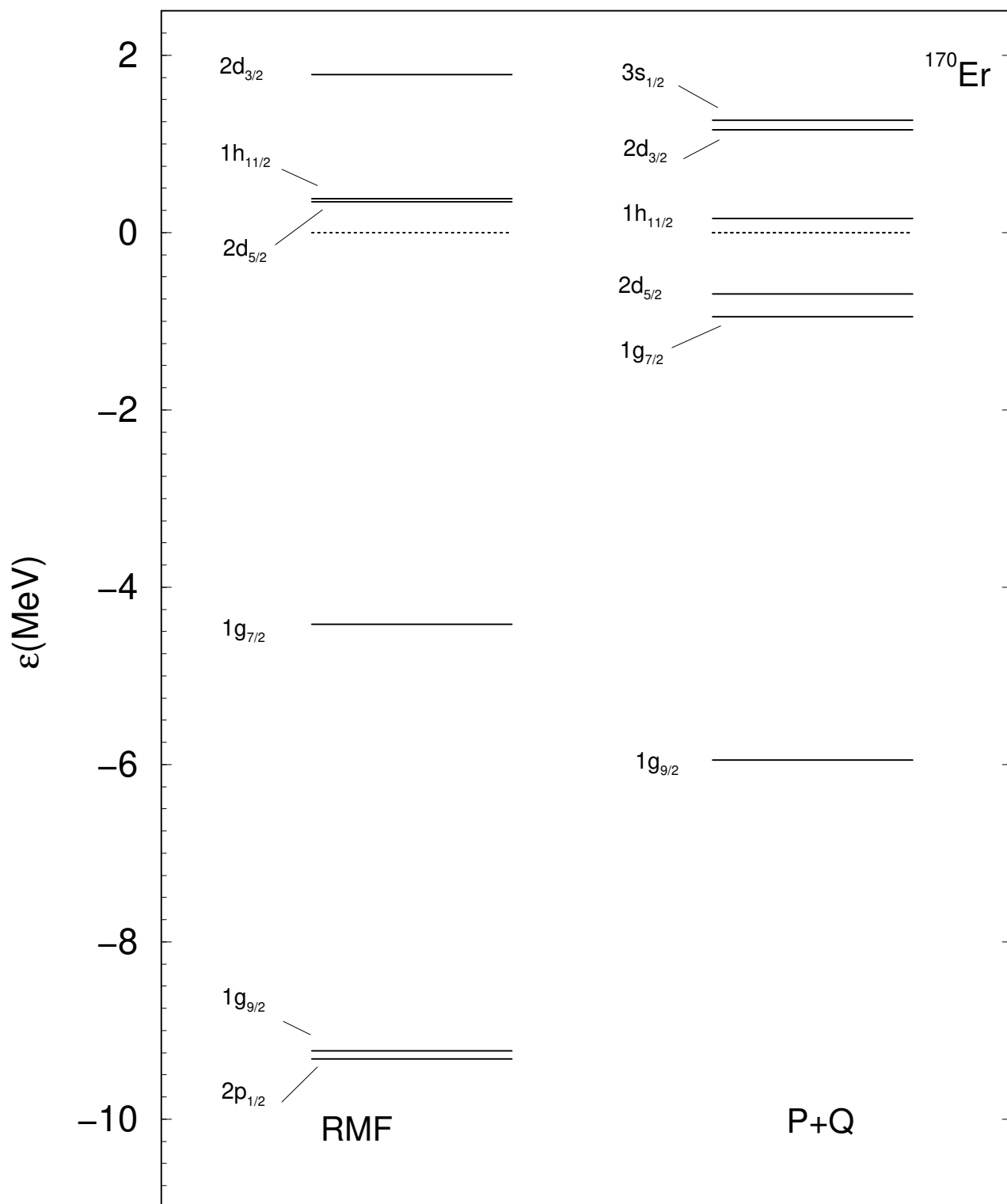


Fig. 5

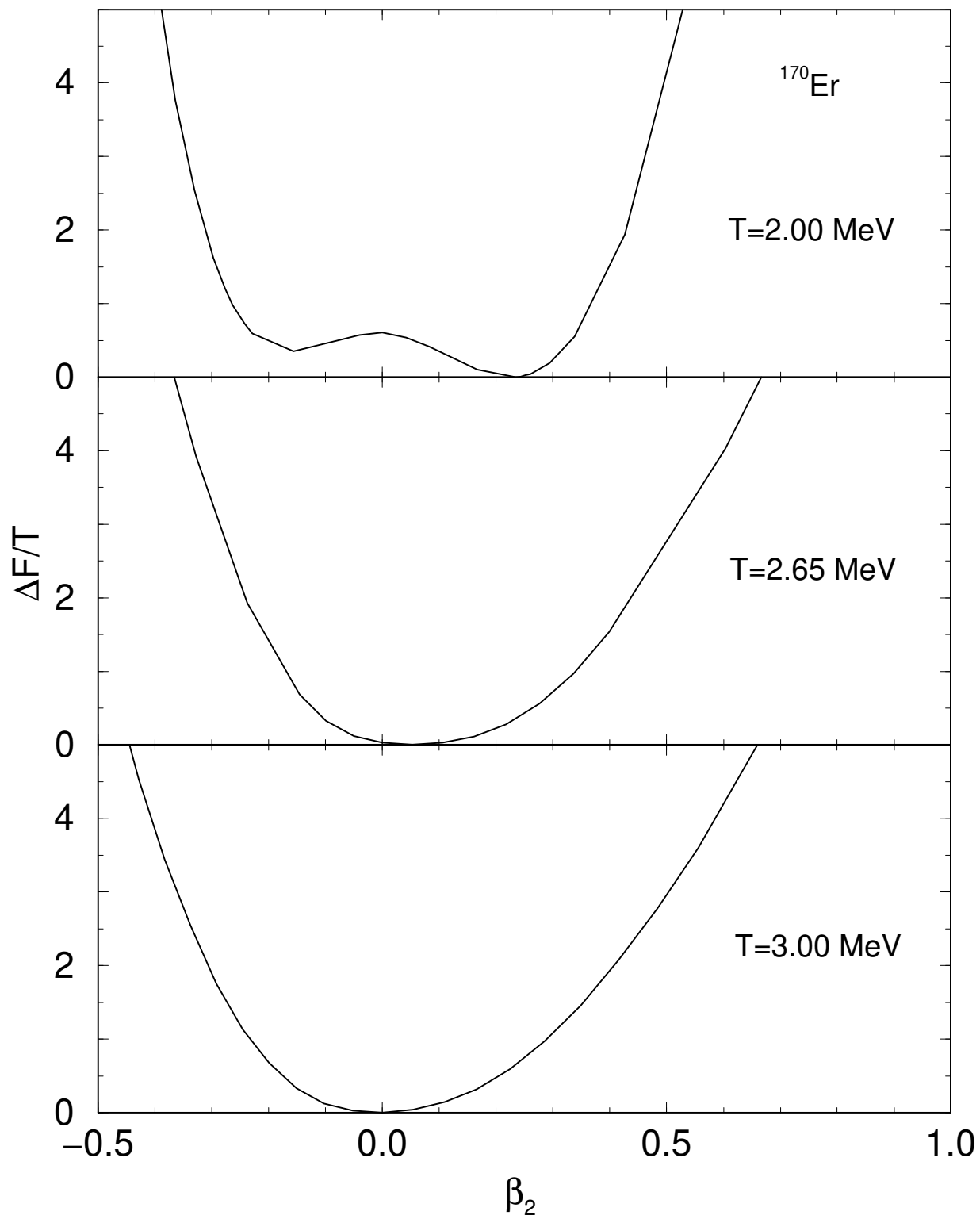


Fig. 6

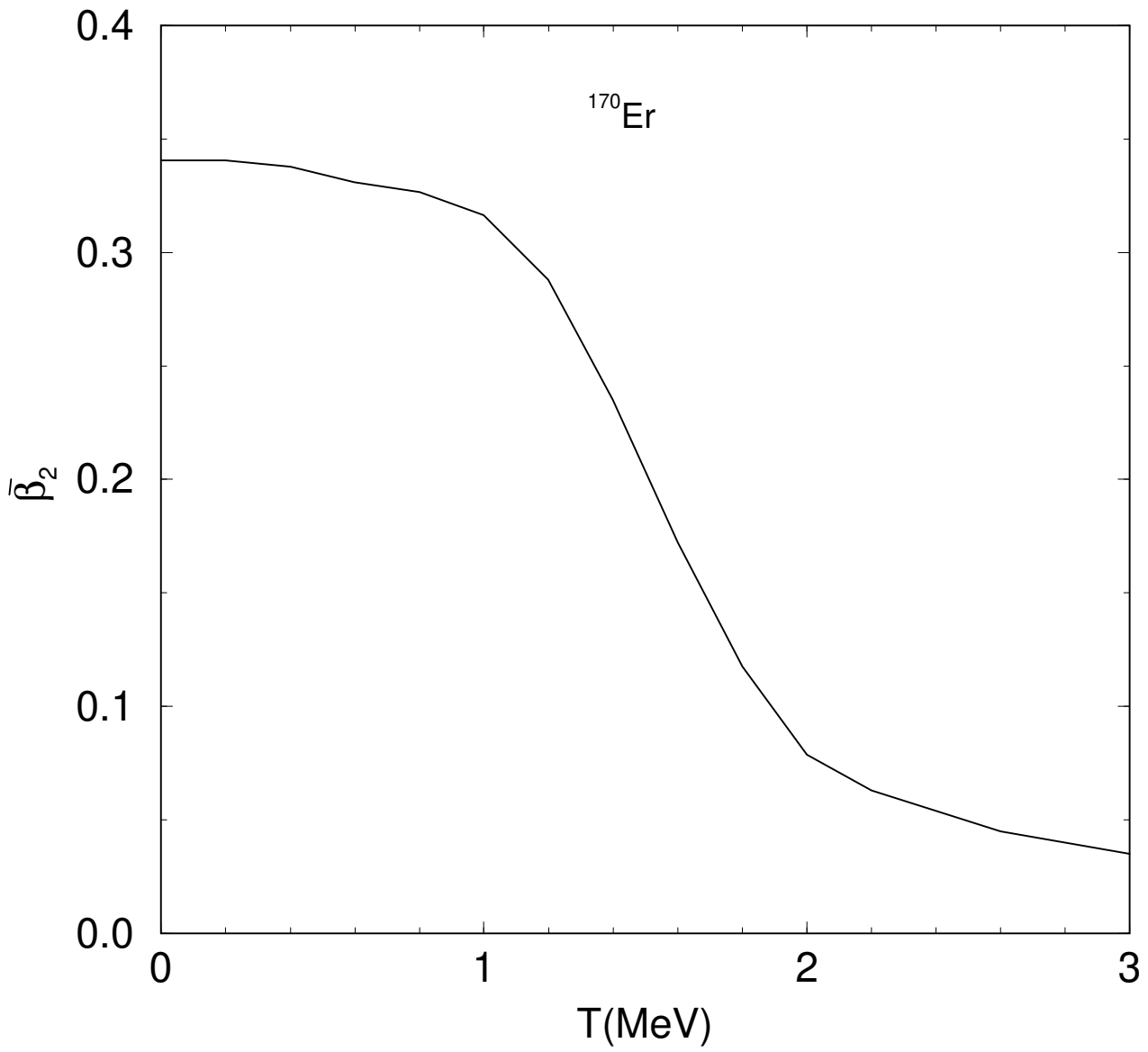


Fig. 7

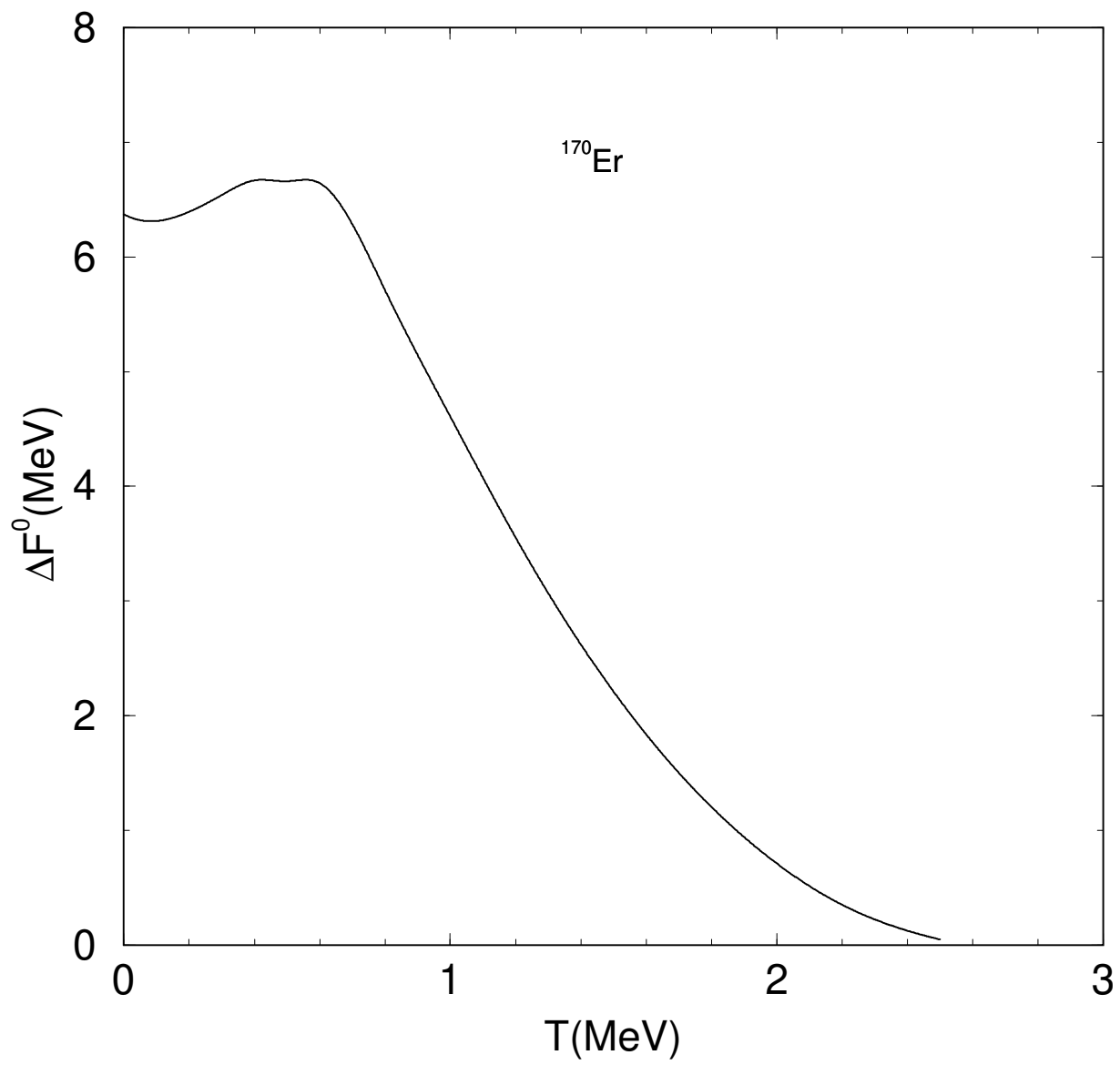


Fig. 8

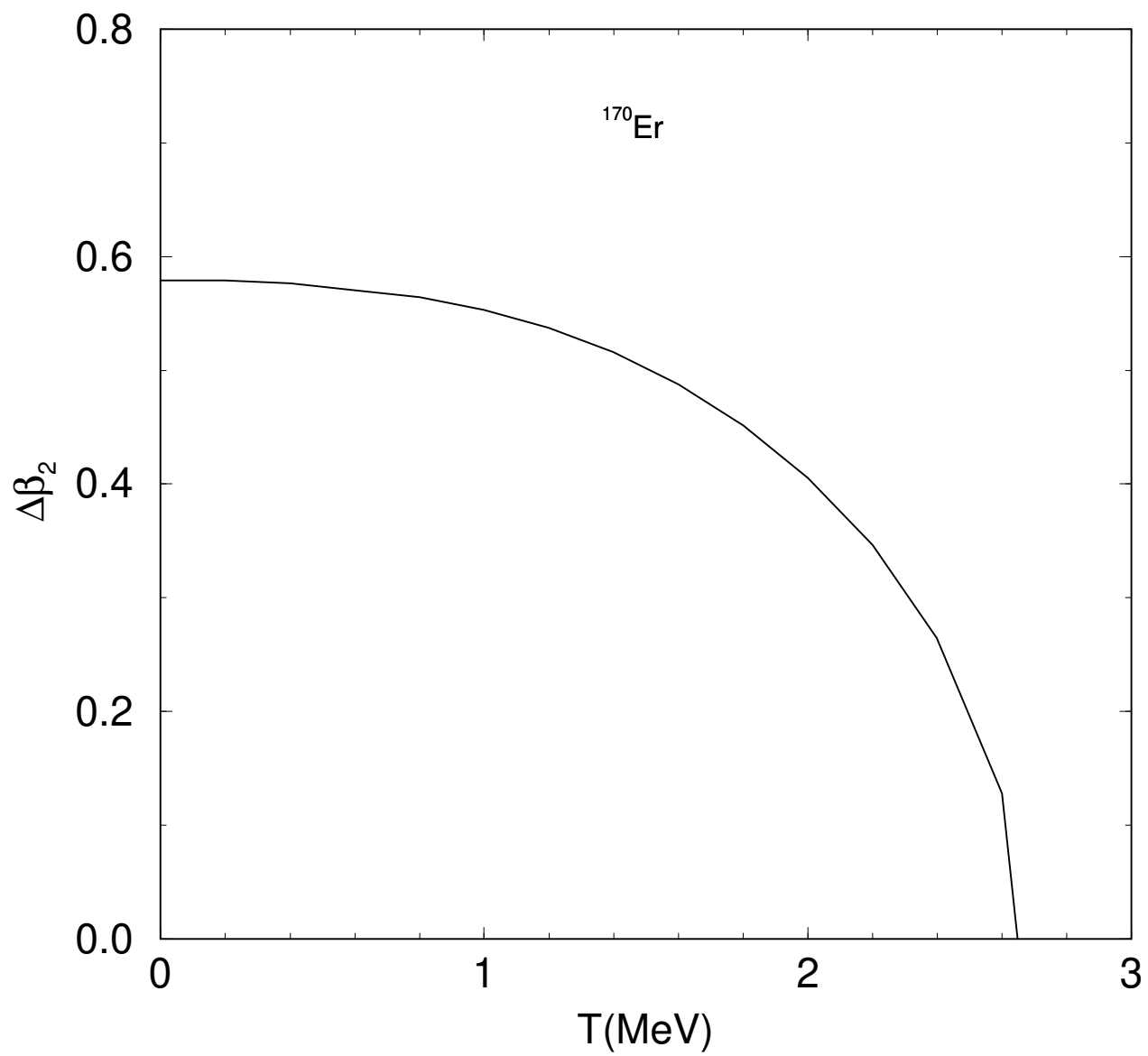


Fig. 9

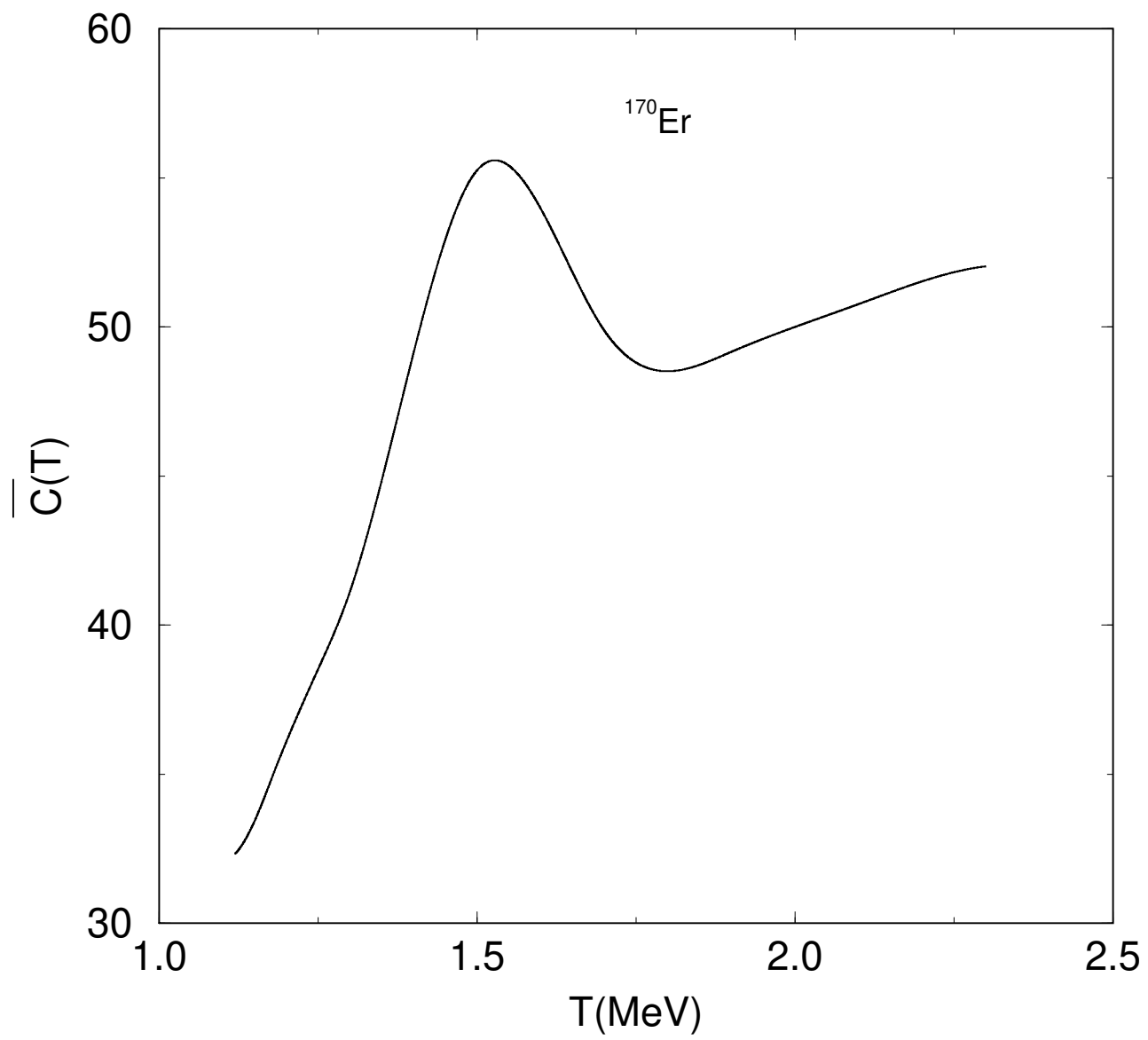


Fig. 10

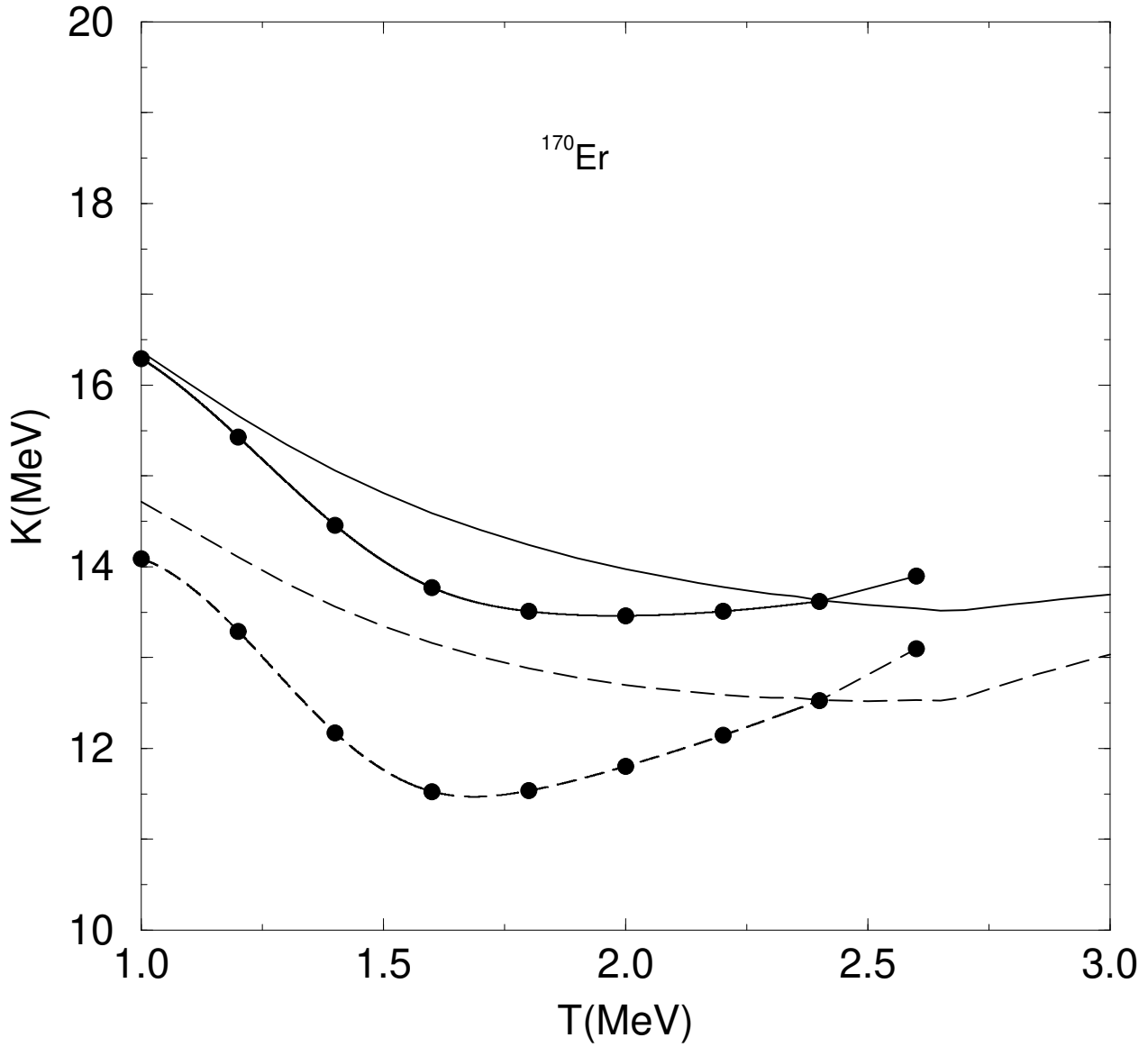


Fig. 11